

**DETERMINATION OF THE EFFECTIVE DIELECTRIC CONSTANT OF THE LUNAR SURFACE BASED ON THE RADAR ECHO INTENSITY OBSERVED BY THE KAGUYA.** A. Kumamoto<sup>1</sup>, K. Ishiyama<sup>1</sup>, T. Kobayashi<sup>2</sup>, S. Oshigami<sup>3</sup>, and J. Haruyama<sup>4</sup>, <sup>1</sup>Graduate School of Science, Tohoku University (Aoba, Aramaki, Aoba, Sendai 980-8578, Japan. E-mail: kumamoto@stpp.gp.tohoku.ac.jp), <sup>2</sup>Korea Institute of Geoscience and Mineral Resources, <sup>3</sup>National Astronomical Observatory of Japan, <sup>4</sup>Institute of Space and Astronautical Science, Japan Aerospace Exploration Agency.

**Introduction:** In the planetary radar observation, echo power and delay time depend on the effective dielectric constant, or equivalent dielectric constant including the voids in the planetary uppermost media. As for the Moon, because there is almost no material whose dielectric constant is far from the basalt rocks, the effective dielectric constant of the lunar uppermost media is considered to depend mainly on their porosity. So if we can determine the effective dielectric constant of the lunar uppermost media, we can derive their bulk density, or density including the voids. According to the previous study based on the investigations of Apollo samples [1], the bulk density  $\rho_{bulk}$  can be derived from the effective dielectric constant  $\epsilon_r$  as follows:

$$\rho_{bulk} [\text{g/cm}^3] = \frac{\log_{10} \epsilon_r}{\log_{10} 1.919} \quad (1)$$

The reflectivity of the electromagnetic waves between two media depends not only on their dielectric constants but also on the roughness of the boundary between them. In our previous analysis [2], we determined the dielectric constant of the lunar uppermost media by using the intensity of the radar echo measured by Kaguya Lunar Radar Sounder (LRS) [3, 4, 5, 6], and the surface roughness parameters derived from Digital Terrain Model (DTM) based on Kaguya Terrain Camera (TC) [7]. Also in other study [8], we have determined the effective dielectric constant of the uppermost basalt layers in several regions by using the apparent radar depth and actual depth of the subsurface boundaries around the impact craters measured by Kaguya. The derived dielectric constant was less than that of the Apollo rock samples, which suggested that some part of the porosity was due to the macro cracks made by the meteorite impacts. In this study, we have compared the effective dielectric constant derived from the surface echo intensity with that derived from the apparent radar depth.

**Analyses Method:** The global distributions of the echo powers in a frequency range of 4-6 MHz were derived from the Kaguya/LRS dataset. The Kaguya spacecraft moved along the polar orbit with an altitude of about 100 km. In order to achieve enough range resolution, Kaguya/LRS transmitted chirp pulse with a bandwidth of 2MHz. The range resolution of LRS in vacuum is therefore 75m. The transmission power of

Kaguya/LRS was 800 W [3, 4, 5, 6]. In this study, we have used the intensity of off-nadir echoes in an incident angle less than 15 degree, which arrive after the nadir echo. We should note that the echoes after the nadir echo consists of various components such as off-nadir surface echoes, volume scatters from the materials below the surface, and echoes from the subsurface reflectors. In this study, we assumed that most of them was off-nadir surface echoes. The median of off-nadir echo intensities were derived in 120 x 60 areas divided by 3 degree longitude x 3 degree latitude grid.

In addition, we have also derived the global distribution of the surface roughness parameters. The RMS height  $\nu$ , or Allan deviation of the surface height, can be obtained by

$$\{\nu(\Delta x)\}^2 = \langle \{z(x+\Delta x) - z(x)\}^2 \rangle, \quad (2)$$

where  $z(x)$  is height of the surface derived from the Kaguya TC/DTM,  $\Delta x$  is baseline length, and  $\langle \rangle$  denotes the average. If we assume the self-affine surface model, the roughness parameters  $H$  and  $s$  can be obtained by the least square fitting of the RMS heights to

$$\nu(\Delta x) = s \Delta x^H, \quad (3)$$

in a baseline length range from 30 m to 30 km. The roughness parameters were derived in 120 x 60 areas divided by 3 degree longitude x 3 degree latitude grid. As for Hurst exponent  $H$ , the global distribution has been reported based on the Lunar Reconnaissance Orbiter (LRO) laser altimeter data [9].

The off-nadir surface echo power can be calculated based on the radar equation. Assuming Kirchhoff Approximation (KA), the backscattering coefficient in the radar equation can be obtained from the roughness parameters  $H$  and  $s$ , and the dielectric constant [cf. 10, 11, 12]. Using the roughness parameters  $H$  and  $s$  obtained by Kaguya TC/DTM and changing the assumed dielectric constant, we can calculate the expected off-nadir surface echo powers and compare them with observed off-nadir surface echo power. Based on the comparison, we can determine most plausible dielectric constant.

**Results:** The global distributions of roughness parameters,  $H$  and  $\log_{10} s$ , were obtained based on TC/DTM. The Hurst exponent  $H$  is less than 0.5 in the maria, and about 0.9 in the highlands. The parameter  $s$  is about 0.2 in the maria, and about -0.5 in the high-

lands. The global distribution of  $H$  is similar with that based on LRO [9]. By applying the analysis method mentioned above, we could obtain the observed and calculated surface echo powers. Based on them, we could estimate the effective dielectric constant of the lunar uppermost media in  $120 \times 60$  areas divided by 3 degree longitude  $\times$  3 degree latitude grid. In our previous studies, the effective dielectric constant estimated based on the apparent radar depth were in a range of 2.8-5.5 around  $43^\circ\text{W}$ ,  $26^\circ\text{S}$ , 2.5-32.1 around  $17^\circ\text{E}$ ,  $24^\circ\text{N}$ , and 4.2-18 around  $17^\circ\text{E}$ ,  $21^\circ\text{N}$  based on the apparent radar depth measurements [8]. The observed and calculated echo intensities in  $43.5 \pm 1.5^\circ\text{W}$ ,  $25.5 \pm 1.5^\circ\text{S}$ , and in  $16.5 \pm 1.5^\circ\text{E}$ ,  $19.5 \pm 1.5^\circ\text{N}$  are indicated in Figures 1 and 2. The effective dielectric constants and the bulk density estimated in this study are  $\epsilon_r = 2.7$  and  $\rho_{\text{bulk}} = 1.5 \text{ g/cm}^3$  in  $43.5 \pm 1.5^\circ\text{W}$ ,  $25.5 \pm 1.5^\circ\text{S}$ ,  $\epsilon_r = 2.2$  and  $\rho_{\text{bulk}} = 1.2 \text{ g/cm}^3$  in  $16.5 \pm 1.5^\circ\text{E}$ ,  $22.5 \pm 1.5^\circ\text{N}$ , and  $\epsilon_r = 2.5$  and  $\rho_{\text{bulk}} = 1.4 \text{ g/cm}^3$  in  $16.5 \pm 1.5^\circ\text{E}$ ,  $19.5 \pm 1.5^\circ\text{N}$ .

**Discussion:** In comparison between observed and calculated echo intensities, we found mismatch in an incident angle range below 3 degree. We infer that it is due to the interferences of echoes from the boundaries between the multiple thin layers just below the surface. In this analysis, we used off-nadir echo intensities in an incident angle range from 5 to 15 degree.

The effective dielectric constant estimated in this study are also less than those of the Apollo rock samples, which support the hypothesis of the high porous uppermost basalt layer suggested in the previous studies [8]. The effective dielectric constants estimated in this study are close to the lower limit of the possible dielectric constant range estimated in the previous studies. They were determined based on the depths of the haloed craters which excavate the subsurface basalt layers below the uppermost basalt layers. It can be therefore suggested that the depths of the subsurface boundaries between the uppermost basalt layers and the lower basalt layers are almost close to the depths of the haloed craters due to the stiffness of the lower basalt layers. The effective dielectric constant in  $16.5 \pm 1.5^\circ\text{E}$ ,  $19.5 \pm 1.5^\circ\text{N}$  estimated in this study is a little different from that estimated in the previous studies. The dielectric constant range of 4.2-18 was estimated based on the assumption that the dielectric constant is almost constant in the same lava flow unit. It might suggest that we should consider inhomogeneity of the effective dielectric constant even in the same lava flow. Because we use the median of the off-nadir echo intensities in this study, the estimated dielectric constant can not be affected by the minor component.

We could perform the cross calibration between the two different determination methods of the dielectric constant of the lunar uppermost media. We will be able to apply the determination method used in this study in wider area on the lunar surface because it does not need impact craters, which are needed in the previous studies [8].

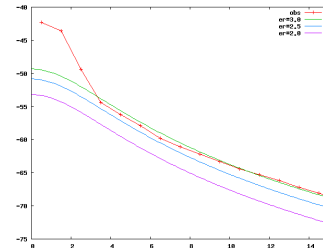


**Figure 1:** Observed (red curve) and calculated echo powers (other curves) as a function of incident angle in  $43.5 \pm 1.5^\circ\text{W}$ ,  $25.5 \pm 1.5^\circ\text{S}$ . The dielectric constant of 3.0 (green curve), 2.5 (blue curve), and 2.0 (magenta curve) are assumed in the calculation.

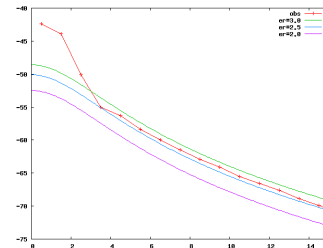


**Figure 2:** Observed (red curve) and calculated echo powers (other curves) as a function of incident angle in  $16.5 \pm 1.5^\circ\text{E}$ ,  $19.5 \pm 1.5^\circ\text{N}$ . The format is the same with that of Figure 1.

**Acknowledgements:** The authors wish to express their sincere thanks to all of the Kaguya team member. The authors also wish to express their deep gratitude to Prof. Takayuki Ono, Principle Investigator of Kaguya/LRS, who passed away on December 21, 2013.

**References:** [1] Carrier, W. D. III et al. (1991) Lunar source book: A user's guide to the Moon, 475-594. [2] Kumamoto, A. et al. (2013), 44th LPSC, #1950. [3] Ono, T. and Oya, H. (2000) EPS, 52, 629-637. [4] Ono, T. et al. (2008) EPS, 60, 321-332. [5] Ono, T. et al. (2009) Science, 323, 5916, 909, doi:10.1126/science.1165988. [6] Ono, T. et al. (2010) SSR, 154, 145-192, doi:10.1007/s11214-010-9673-8. [7] Haruyama, J. et al. (2008) EPS, 60, 243-255. [8] Ishiyama, K. et al. (2013), JGRE, 118, 1453-1467, doi:10.1002/jgre.20102. [9] Rosenburg, M. A. et al. (2011) JGRE, 116, E02001, doi:10.1029/2010JE003716. [10] Franceschetti, G. et al. (1999) IEEE Trans. Antennas Propagat., 47, 9, 1405-1415. [11] Shepard, M. K., and Campbell, G. A. (1999) Icarus, 141, 156-171. [12] Bruzzone, L. et al. (2011) Proc. IEEE, 99, 5, 837-857, doi: 10.1109/JPROC.2011.2108990.